

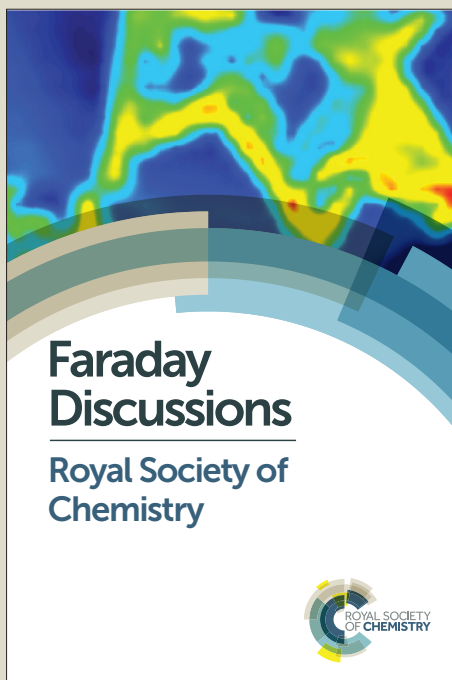
# Faraday Discussions

Accepted Manuscript



This manuscript will be presented and discussed at a forthcoming Faraday Discussion meeting. All delegates can contribute to the discussion which will be included in the final volume.

**Register now to attend!** Full details of all upcoming meetings: <http://rsc.li/fd-upcoming-meetings>



This is an *Accepted Manuscript*, which has been through the Royal Society of Chemistry peer review process and has been accepted for publication.

*Accepted Manuscripts* are published online shortly after acceptance, before technical editing, formatting and proof reading. Using this free service, authors can make their results available to the community, in citable form, before we publish the edited article. We will replace this *Accepted Manuscript* with the edited and formatted *Advance Article* as soon as it is available.

You can find more information about *Accepted Manuscripts* in the [Information for Authors](#).

Please note that technical editing may introduce minor changes to the text and/or graphics, which may alter content. The journal's standard [Terms & Conditions](#) and the [Ethical guidelines](#) still apply. In no event shall the Royal Society of Chemistry be held responsible for any errors or omissions in this *Accepted Manuscript* or any consequences arising from the use of any information it contains.



## Faraday Discussion

## ARTICLE

## A Theoretical Consideration of Ion Size Effects on the Electric Double Layer and Voltammetry of Nanometer-sized Disk Electrodes

Received 00th January 20xx,  
Accepted 00th January 20xx

DOI: 10.1039/x0xx00000x

[www.rsc.org/](http://www.rsc.org/)

Yu Gao, Yuwen Liu and Shengli Chen\*

Considering that the EDL structure may significantly impact the mass transport and charge transfer kinetics at interfaces of nanometer-sized electrodes, while the EDL structures could be altered by the finite sizes of electrolyte and redox ions, the possible effects of ion sizes on the EDL structures and voltammetric responses of nanometer-sized disk (nanodisk) electrodes are investigated. Modified Boltzmann and Nernst-Planck (NP) equations, which include the influence of the finite ion volumes, are combined with the Poisson equation and modified Butler-Volmer equation to gain knowledge on how the finite sizes of ions and the nanometer sizes of electrodes may couple with each other to affect the structures and reactivities of nanoscale electrochemical interface. Two typical ion radii, 0.38 nm and 0.68 nm, which could represent the sizes of the commonly used aqueous electrolyte ions (e.g., the solvated  $K^+$ ) and the organic electrolyte ions (e.g., the solvated  $TEA^+$ ) respectively, are considered. The finite size of ions can result in decreased screening of electrode charges, therefore magnifies the EDL effects on the ion transport and the electron transfer at electrochemical interfaces. This finite size effect of ions becomes more pronounced for larger ions and at smaller electrodes as the electrode radii is larger than 10 nm. For electrodes with radii smaller than 10 nm, however, the ion size effect could be less pronounced with decreasing the electrode size. This can be explained in terms of the increased edge effect of disk electrodes at nanometer scales, which could relax the ion crowding at/near the outer Helmholtz plane. The conditions and situations under which the ion sizes may have significant effect on the voltammetry of electrodes are discussed.

### Introduction

Understanding the structures and processes at nanoscale electrochemical interfaces is of significance in diverse areas such as energy conversion, application of scanning probe microscopies in electrolyte solutions, electrochemical fabrication and characterization of nanomaterials, and so on.<sup>1-2</sup> Nanometer-sized electrodes (nanoelectrodes) provide model systems to investigate the electrochemistry at nanoscale interfaces. When the electroactive sizes of electrodes or the structural units of electrodes are reduced to nanoscales so that they are comparable with the characteristic lengths of electric-double-layers (EDLs), some distinct interfacial features which are inappreciable at macro/microscale electrodes may arise, one of which is the significantly enhanced EDL effects on the charge transfer kinetics and transport dynamics even in the presence of excess of supporting electrolytes. Such EDL effects make the electrode sizes impact the electrochemical responses not only quantitatively but also qualitatively. During the past two decades, there have been numerous theoretical and experimental studies demonstrating the distinct EDL

effects at nanometer-sized electrodes.<sup>1-10</sup>

In previous theoretical studies<sup>1,3,4</sup>, the EDL effects on the electrochemistry of nanoelectrodes have been mostly modelled with the continuum equations which neglect the sizes (volumes) of electrolyte ions, for examples, the conventional Boltzmann equation for ion distribution at equilibrium interfaces and the Nernst-Planck equation for ion transport in dynamic interface. Whether these continuum equations are applicable or not remains a question at present. Krapf et al.<sup>6</sup> have observed a strong nonlinear dependence of the limiting current on the concentration of electroactive ions at hemispherical electrodes smaller than 10 nm in diameters, which seemed to challenge the validity of the continuum equations at such small electrodes. The experimental observation by Sun et al.<sup>7</sup> have shown an approximately linear dependence of the limiting current on the concentration of reactants at disk electrodes smaller than 10 nm, which deviates from the prediction of diffusion-based mass transport equation, but can be reasonably explained with the continuum Poisson-Nernst-Planck equations.

It is known that the sizes of ions would visibly impact the EDL structure when the concentrations of electrolyte or redox ions are considerably high or their sizes are considerably large, so that significant crowding of ions in the region near electrode surface occurs.<sup>11-16</sup> One of the recent strategies in developing high performance energy and electronic systems is

\* Key Laboratory of Analytical Chemistry for Biology and Medicine (Ministry of Education), Hubei Key Laboratory of Electrochemical Power Sources, Department of Chemistry, Wuhan University, Wuhan 430072, China. Fax: 027-68754693; Tel: 027-68754693; E-mail: [slchen@whu.edu.cn](mailto:slchen@whu.edu.cn)

to use media that have high electrochemical windows, for examples, organic solvents,<sup>17</sup> ionic liquids<sup>18-20</sup> and molten salts<sup>21</sup>. The large-size cations such as tetra-alkylammonium (TEA<sup>+</sup>), imidazolium and phosphonium, and anions such as bis(trifluoromethane sulfonyl)imide (TFSI<sup>-</sup>) and CF<sub>3</sub>SO<sub>3</sub><sup>-</sup> are the common components of ionic liquids or organic electrolytes; while the ionic liquids and molten salts are typical concentrate media. Recently, the highly concentrated aqueous solution of LiTFSI (>20 M) has been shown to enable potential window as high as 3.0 V<sup>22</sup>.

The application of nanoscopic electrode materials and the concentrated and large-size electrolytes in modern energy technologies make it necessary to investigate the ion size effects on the structures and reactivity of nanoscale electrochemical interfaces. It could provide knowledge for designing new energy systems and/or to improve the current systems. As known from previous studies, the electron transfer and ion transport processes would be more pronouncedly impacted by the EDL structures at nanometer-sized electrodes,<sup>1-8,10</sup> while the ions with large sizes can significantly impact the EDL structures.<sup>11-16</sup> Therefore, the sizes of electrolyte ions should also impact the reactivity at nanoscale electrochemical interfaces.

In this paper, using nanometer-sized disk (nanodisk) electrodes as models, we study how the nanometre size effect of electrodes and the finite size effect of ions can be coupled to affect the EDL structure and reactivity at nanoscale electrochemical interface. The approach by Bikerman et al<sup>11, 23-26</sup> for treating the finite volume effect of ions is adopted to modify the conventional Boltzmann and Nernst-Planck (NP) equations, which, together with the Poisson equation and the modified Butler-Volmer equations, are used to gain knowledge on how the finite size effect of ions may be altered by the nanometer sizes of electrodes. It is shown that the ion size effect become more pronounced for larger ions and at smaller electrodes as the electrode radii are larger than 10 nm. For electrode with radii smaller than 10 nm, however, the ion size effect becomes less pronounced at smaller electrodes due to the increased edge effect of disk electrodes at nanometer scales, which could relax the ion crowding at/near the outer Helmholtz plane.

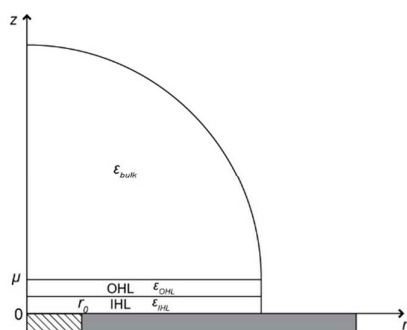
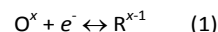


Fig. 1 Schematic illustration of the geometric model used for nanodisk electrode interface

## Model and simulation

We consider the following outer-sphere one-electron reduction reaction in solution containing a symmetric electrolyte of M<sup>+</sup>N<sup>-</sup> at a nanodisk electrode with electroactive radius of r<sub>0</sub> which is embedded by an insulation sheath (e.g., glass) of infinite thickness.



The interface at the nanodisk electrodes is geometrically modelled with a cylindrical coordinate system of axial symmetry containing radial coordinate *r* and normal coordinate *z* (Fig. 1). The center of the electrode surface is set as the origin of the coordinate system. Since we are interested mainly in how the ion size effect could be different at nanometer-sized electrodes, the complexities from other factors are ignored for simplicity. Therefore, it is assumed that the compact EDL form on the surface of the insulation sheath as well as electrode, with the same thickness *μ*; no free charge resides in the compact EDL, that is, none of ions in the system chemically adsorbs on the electrode surface; the compact EDL can be into two regions, namely, the outer Helmholtz layer (OHL) and inner Helmholtz layer (IHL), which are composed of closely packed solvent molecules and solvated ions respectively;<sup>4</sup> the relative dielectric constant of the media in the IHL and OHL (*ε*<sub>IHL</sub> and *ε*<sub>OHL</sub>) are different from that in the solution due to the dielectric saturation effect under the strong electric field in the EDL;<sup>4</sup> all the ions have the same plane of closest approach at the outer boundary of the OHL, the so-called outer Helmholtz plane (OHP); the O<sup>x</sup> and R<sup>x-1</sup> have the same diffusion coefficient (*D* = 10<sup>-9</sup> m<sup>2</sup>s<sup>-1</sup>); and all ions have the same radius (*r*<sub>ion</sub>).

The finite size effect of electrolyte ions was first considered for the equilibrium EDL in the case of symmetric electrolyte by Bikerman in early 1940s.<sup>11</sup> Based on the lattice gas models which consider the ions as discrete cells of certain volumes, the finite sizes of ions result in a modified entropic contribution of ion concentration to the Helmholtz free energy.<sup>11-13</sup> These treatments have also been extended to more general cases, for examples, for unsymmetrical electrolytes<sup>23</sup> and EDL dynamics<sup>24</sup>. Various treatments to the finite size effects of ions can be generalized by adding an excess term to the chemical potential of the corresponding ions, *μ*<sub>*i*</sub><sup>ex</sup>, that is<sup>23-26</sup>

$$\mu_i = RT \ln c_i + z_i F \phi + \mu_i^{ex} \quad (2)$$

in which *z<sub>i</sub>*, *c<sub>i</sub>* and *μ<sub>i</sub>* are the charge, local concentration and chemical potential of the *i*<sup>th</sup> ion, *φ* is the local electrostatic potential, and *R*, *T* and *F* have their usual meanings. The excess chemical potentials can be expressed as

$$\mu^{ex} = -k_B T \ln(1 - \Phi) \quad (3)$$

in which *Φ* is the volume fraction of all ions (anions + cations) in the solution, which can be expressed as

$$\Phi = \sum c_i / c_{max} \quad (4)$$

where *c*<sub>max</sub> = 1/8*r*<sub>ion</sub><sup>3</sup> *N*<sub>A</sub> is the maximum concentration the ions can reach, and *N*<sub>A</sub> is the Avogadro constant. Based on Eq. 2-4, a modified Boltzmann equation for equilibrium ion distribution

can be obtained by using the condition that the chemical potential is uniform at the interface and in the solution. That is [11-13],

$$c_i = \frac{c_i^0 e^{-(z_i F \phi / RT)}}{1 + 2c_i^0 \sinh^2(F \phi / 2RT) / c_{\max}} \quad (5)$$

in which  $c_i^0$  is the bulk concentration of the ion. This is also called the Fermi distribution equation, which will reduce to the conventional Boltzmann distribution equation as the value of  $\Phi$  approaches zero.

The chemical potential expression of Eq. 2 can also be used to treat the finite size effect on the ion transport at interface where redox reactions take place, by modifying the conventional Nernst-Planck (NP) equation. For steady-state ion transport in cylindrical coordinate system, we have

$$\left( \frac{\partial c_i}{\partial t} \right) = -\frac{1}{r} \nabla (r J_i) = -\frac{1}{r} \nabla \cdot \left( \frac{D_i c_i}{RT} r \nabla \mu_i \right) = 0 \quad (6)$$

in which  $J_i$  and  $D_i$  refer to the flux and diffusion coefficient of the  $i^{\text{th}}$  ion. In cylindrical coordinate system, the gradient operator  $\nabla = (\partial/\partial r + \partial/\partial z + 1/r)$ . Combination of Eq. 2-4 and Eq. 6 leads to

$$\nabla \cdot D_i \left( r \nabla c_i + \frac{z_i F c_i}{RT} r \nabla \phi + \frac{c_i}{c_{\max} (1 - \Phi)} r \nabla \sum_i c_i \right) = 0 \quad (7)$$

Eq. 7 will reduce to the conventional NP equation as the value of  $\Phi$  approaches zero. To get the equilibrium distribution or the transport rate of an ion, Eq. 5 or 7 has to be solved together with the Poisson equation which has the following form in cylindrical coordinate system,

$$\rho = \frac{1}{r} \varepsilon_0 \nabla \cdot (-\varepsilon r \nabla \phi) \quad (8)$$

where  $\rho$  refers to the local charge density,  $\varepsilon$  and  $\varepsilon_0$  are the relative dielectric constant and the permittivity of a vacuum.

Eq. 5 and 7 should be solved in the domain of  $z > \mu$ , where  $\mu = l_{\text{IHP}} + l_{\text{OHP}}$  is the thickness of the compact region of EDL, and  $l_{\text{IHP}}$  and  $l_{\text{OHP}}$  are the thickness of the IHL and OHL respectively. The Poisson equation (Eq. 8) should be solved in the domain of  $z > 0$ . To solve these equations, the following boundary conditions are used.

$$r = \infty \text{ or } z = \infty : \phi = 0, \nabla \phi = 0 \text{ and } c_i = c_i^0 \quad (9)$$

$$-r_0 \leq r \leq r_0 \text{ and } z = 0 : \phi = E \quad (10)$$

$$-r_0 \leq r \leq r_0 \text{ and } z = \mu : \phi = \phi_{\text{OHP}} \quad (11)$$

$$-r_0 \leq r \leq r_0 \text{ and } z = \mu : J_i = -m_j \frac{i}{nF} \quad (12)$$

$$r > r_0 \text{ (or } r < -r_0) \text{ and } z = \mu : J_i = 0 \quad (13)$$

where  $E$  refers to the electrode potential,  $\phi_{\text{OHP}}$  is the electrostatic potential at OHP,  $i$  is the current density on electrode surface,  $m_j$  is a integer constant taking values +1, -1 and 0 for species  $R^{x-1}$ ,  $O^x$ , and the inert electrolyte ions respectively. The reduction current is defined as positive here. For simplicity, we use the Butler-Volmer (BV) model to describe the kinetics of charge transfer reaction at electrode surface, that is

$$\frac{i}{F} = k^0 \left\{ c_{O^x} \exp\left(\frac{-F(E - E^0 - \phi_{\text{OHP}})}{2RT}\right) - c_{R^{x-1}} \exp\left(\frac{F(E - E^0 - \phi_{\text{OHP}})}{2RT}\right) \right\} \quad (14)$$

in which  $k^0$  and  $E^0$  refer to the standard rate constant and the standard equilibrium potential of reaction (1). The Eq. 14 is a modified form of the conventional BV equation to include the effect of EDL on the electron transfer kinetics, specifically, the term " $E - E^0$ " in the normal BV equation is replaced by " $E - E^0 - \phi_{\text{OHP}}$ ".

For comparison, we also consider the simple situation when the mass transport and electron transfer processes are not affected by the EDL structure. In this case, the steady-state diffusion equation including the ion size effect is used to describe the mass transport of redox species, that is,

$$\nabla \cdot D_i \left( r \nabla c_i + \frac{c_i}{c_{\max} (1 - \Phi)} r \nabla \sum_i c_i \right) = 0 \quad (15)$$

and the term " $E - E^0 - \phi_{\text{OHP}}$ " in Eq. 14 should be changed to " $E - E^0$ ". Similarly, Eq. 15 will reduce to the conventional diffusion equation when  $\Phi$  is zero.

The equations are solved numerically using the finite-element-method package of Comsol Multiphysics. In the computations, the bulk concentrations of  $O^x$ ,  $R^{x-1}$ ,  $M^+$  and  $N^-$  are 0.01, 0, 0.1 and 0.1 mol·L<sup>-1</sup> respectively; the diffusion coefficients for all ions are all 1×10<sup>-5</sup> cm<sup>2</sup>·s<sup>-1</sup>; the dielectric constants are 6, 40, and 78.3 respectively in the IHL, OHL and region outside the compact double layer; the thicknesses of IHL and OHL are 0.3 nm and 0.29 nm respectively; the standard rate constant is 1.0 cm/s; the standard electrode potential is 0 V with respect of the potential of zero charge (PZC); and T=298.15K.

## Results and Discussion

### Effect of electrolyte ion sizes on the equilibrium EDL structures at nanodisk electrodes.

We mainly consider two sizes of electrolyte ions, 0.38 and 0.68 nm, which represent the sizes of the commonly used aqueous electrolyte ions, e.g., the solvated  $K^+$ , and the organic electrolyte ions, e.g., the solvated  $TEA^+$ . Since the concentrations of the redox species are very low as compared with the electrolyte ions, we ignore the size effect of the redox species on the EDL structure here.

Fig. 2 shows the electrostatic potential profiles along z-axis away from the OHP (the diffuse part of the interface) at  $r = 0$  as the electrode potential are -0.4 and -1.0 V respectively at electrodes with 10 and 2 nm radii. For electrodes with larger radii, the calculated electrostatic potential profiles (not shown) are very close to that at the 10 nm electrode, regardless of the electrolyte ion sizes. This is because that the EDL structures at electrodes larger than 10 nm in radii are negligibly impacted with electrode sizes. As known from previous studies.<sup>1,4</sup> However, the influence of the EDL structures on the mass transport dynamics and charge transfer kinetics would vary significantly with the electrode sizes as the electrode radii are below 1 μm; more pronounced EDL effect should be seen at smaller electrodes, owing to the increased overlap

between the EDLs and mass transport layers.<sup>1,4</sup> This also will be seen in the next section.

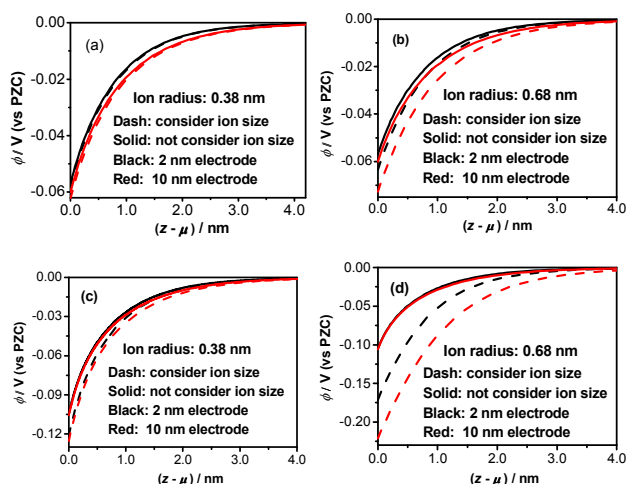


**Fig. 2** Electrostatic potential profiles along  $z$ -axis from OHP at radial coordinate  $r=0$ . Electrode potential: (a, b)  $-0.4$  V; (c, d)  $-1.0$  V. Solid and dash lines: consider and not consider the electrolyte ion sizes.

Only negative electrode potentials are considered because we consider the reduction reaction (1) in this study. It is found that the 0.38 nm size of electrolyte ions have nearly invisible effect on the potential profiles in EDL (Fig. 2a and 2c) and the voltammetric responses of electrodes (shown in next section) positive to  $-0.4$  V. For 0.68 nm ion size, the electrostatic potential profiles are obviously affected by the finite size effect of ion (Fig. 2b and 2d). The finite size of ions makes the electrostatic potentials at the OHP and that in the entire diffuse EDL (dashed line in the figures) higher in magnitudes than that predicted by the conventional Poisson-Boltzmann theory which treats the electrolyte ions as point charges (the solid lines in the figures). The point charge treatment, i.e., ignorance of the finite volumes of ions, could overestimate the concentration of counter ions at and near the OHP, thus over-screen the electrode charge. This can be seen in Fig. 3. When the finite sizes of electrolyte ions are considered according to the modified Poisson-Boltzmann equations (Eq. 5 and 8), the calculated concentration of the counter ion ( $M^+$  here) becomes apparently lower at OHP and in the diffuse EDL. Larger the ion size, lower the concentration of counter ions given by the modified Poisson-Boltzmann equations.

An interesting phenomenon seen from Fig. 2 and 3 is that the effect of ion size becomes less pronounced at the 2 nm electrode than that at the 10 nm electrode. The electrostatic potentials and counter ion concentrations calculated by the modified Poisson-Boltzmann equations (dash lines) show relatively smaller deviation from that predicted by the conventional Poisson-Boltzmann equations (solid lines) at the 2 nm electrode (black lines) than that at the 10 nm electrode (red lines). It is somewhat counter intuitive that the smaller electrode exhibits a lesser size effect than the larger electrode. However, it becomes understandable from the radial concentration profiles of counter ions shown in Fig. 3c and 3d. One can see that the concentration profiles at the 2 nm electrode extend significantly to the region out of the electrode surface ( $r > r_0$ ), which means that the crowding of the counter ions

near the OHP can be relaxed at very small electrodes due to such pronounced edge effect. The edge effect at small electrode offers large space to accommodate the counter ions that approach the OHP. Although the concentration of the counter ion at a given  $r$  coordinate value may be lower at the 2 nm electrode than that at the 10 nm electrode, a higher average concentration value can be obtained at the 2 nm electrode when first integrating the ion concentration over all  $r$  coordinates and then normalizing the integrated value with the electrode radius (or area). Thus, the electrode charge can be more pronouncedly screened by the counter ions at smaller electrode due to the electrode edge effect.

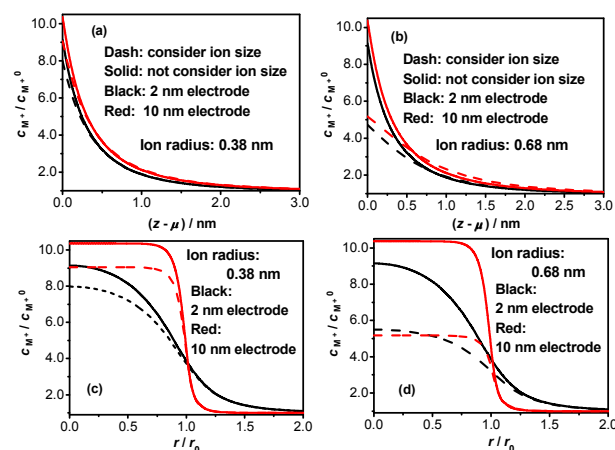


**Fig. 3** Concentration profiles of  $M^+$  ion along  $z$ -axis from OHP at radial coordinate  $r=0$  (a, b) and that along the  $r$ -axis at the OHP ( $z=\mu$ ) (c, d) at electrode potential of  $-0.4$  V. The concentration values are normalized by the corresponding value in the bulk solution. The other details are the same as that in Fig. 2.

As shown in Fig. 4, the radial electrostatic potential profiles also exhibit significant edge effect at the 2 nm electrode, similar to the ion concentration. Again, one can find that the 2 nm electrode exhibits less pronounced ion size effect on the radial profile of electrostatic potential.

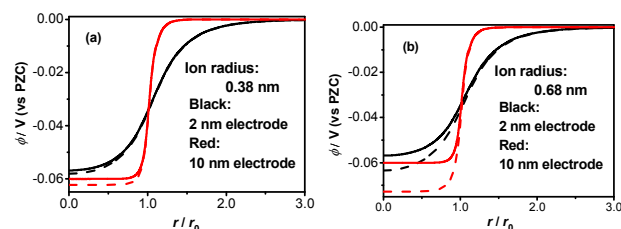


**Fig. 4** Electrostatic potential profiles along the  $r$ -axis at the OHP ( $z=\mu$ ) at electrode potential of  $-0.4$  V. The other details are the same as that in Fig. 2.

#### Effect of finite ion sizes on the voltammetric responses of nanodisk electrodes.

Figure 5 shows The steady-state voltammetric responses of disk electrodes with radii from  $1 \mu\text{m}$  to  $2\text{nm}$  for reaction (1) with  $x=-1$  (anion reduction), calculated by solving the modified Poisson-Nernst-Planck (PNP) equations together with Eq. 14 (considering both the EDL effect and the ion size effect), the conventional PNP equations together with Eq. 14 (considering the EDL effect only), and the diffusion-based transport

equations (Eq. 15) together with the normal BV equation (considering neither the EDL effect nor the ion size effect). For simplicity, we have assumed that all ions in the system have the same sizes when solving the modified PNP equations. It is noted that the voltammetric responses have been normalized by the diffusion limiting current ( $i_{dl}$ ) on the same electrodes. We have found that the voltammetric responses for electrodes of various sizes obtained by solving Eq. 15 are nearly identical to those obtained from the conventional diffusion equation without considering the ion size effect. This is because the ion size affects the voltammetric responses mainly by altering the EDL structure. When the EDL effect is trivial or it is not considered, the effect of the ion size on the voltammetric responses would be negligible.

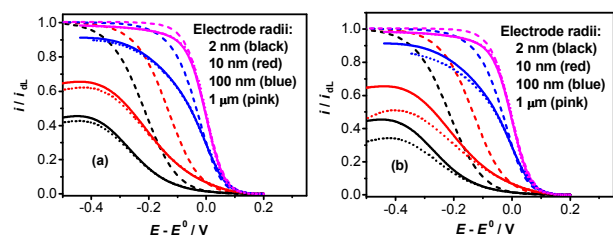


**Fig. 5** Steady-state voltammetric responses of disk electrodes with different radii (distinguished by the line colours) for reduction of an anion with -1 charge, calculated with model including both the EDL and ion size effects (dotted lines), only the EDL effect (solid lines), and neither the EDL nor ion size effect (dash lines). The ion radii are (a) 0.38 nm and (b) 0.68 nm respectively.

The EDL effect decreases the current for the reduction of the anion reactant (comparing the solid and dash lines in Fig. 5). This is due to the mass transport of the reactant ions toward the OHP and the electron transfer kinetics between the electrode and the reactant ions at the OHP are both inhibited by the electrostatic potentials in the diffuse EDL.<sup>1, 3, 4</sup> As has been shown above, the finite size of ions would increase the magnitude of the electrostatic potential in the diffuse EDL due to the reduced screening of electrode charge. Therefore, the ion size effect should result in further decline of the anion reduction current. This can be clearly seen in Fig. 5b for ion with 0.68 nm radius. For ion with 0.38 nm radius, visible influence of ion size on the voltammetric responses is seen only at electrode around 10 nm as the electrode potential is below -0.4 V (Fig. 5a).

The voltammetric responses of the 1  $\mu\text{m}$  electrode shows slight EDL effect in the limiting current region (comparing the solid to dotted lines), indicating that only the mass transport rates of reactant ions are slightly affected by the diffuse EDL at such large electrode. For electrodes with 100 nm and smaller radii, the voltammetric responses are significantly altered by the EDL effect, in both the limiting current and the kinetic regions, indicating that both the mass transport of ions and electron transfer kinetics are strongly affected by the EDL structures. When only the EDL effect is considered, one can

see a simple variation trend that more pronounced EDL effect occurs at smaller electrode.

When the effect of the ion sizes is correlated with the electrode sizes, one can find different variation trends from Fig. 5. As already known, the ion size effect will result in a further current diminishment in addition to the normal EDL effect (comparing the dotted and solid lines). For electrodes with radii between 1  $\mu\text{m}$  and 10 nm, this current diminishment increases in magnitude with decreasing the electrode radius, which is in consistency with the enhanced EDL effect. Upon further reducing the electrode radius from 10 nm, for example, to 2 nm, the current diminishment becomes smaller, although the ordinary EDL effect at the 2 nm electrode remains larger than that at the 10 nm electrode. The reasons for this should be the same as that discussed for the equilibrium EDL. That is, the pronounced edge effect at electrodes smaller than 10 nm can relax the ion crowding caused by the finite volumes.

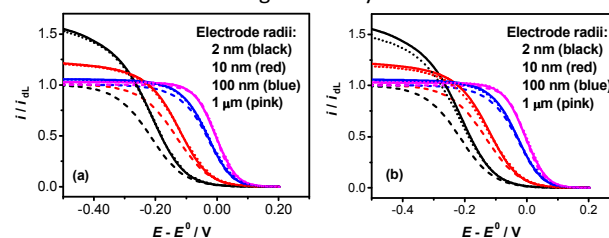


**Fig. 6** Steady-state voltammetric responses of disk electrodes with different radii (distinguished by the line colours) for reduction of a cation with +1 charge. The ion radii are (a) 0.38 nm and (b) 0.68 nm respectively. The other details are the same as that in Fig. 5.

We also have investigated the reduction of the +1-valent cation and the results are shown in Fig. 6. For cation reduction, the electrostatic potentials at the OHP and in the diffuse EDL would accelerate the mass transport of the reactant, while that at the OHP could inhibit the electron transfer kinetics. In most cases, the overall EDL effect should result in increased rates for cation reduction, but the magnitudes of the current increase would be lower than the EDL-induced current decrease for anion reduction at electrodes of the same sizes. This can be seen through comparison of Fig. 6 with Fig. 5. Similar to the anion reduction, the EDL effect also becomes more pronounced at smaller electrode for cation reduction.

One may expect that the EDL-induced current increase would be enhanced by the finite size effect of ions because of the less screened electrostatic interaction, as that seen for the anion reduction in Fig. 5. By comparing the dotted and solid lines in Fig. 6, however, it can be found that the current increase actually becomes less pronounced as the ion size effect is considered. This should be due to that the finite volumes of the redox ions make the actual concentration increase of cation reactant near OHP is lower than that estimated from the electrostatic interaction based on the continuum model. To manifest this effect more clearly, we compare the voltammetric responses of the 2 nm and 10 nm electrodes obtained by considering sizes of both the

electrolyte ions and redox ions and that by considering the sizes of the electrolyte ions but neglecting the sizes of the redox ions. As shown in Fig. 7, the current for cation reduction does show further increase when only the sizes of the electrolyte ions are considered (comparing the dotted and solid lines), which is in consistency with the expectation of magnitude increase of electrostatic potential in the diffuse EDL due to the less screening effect of electrolyte ions to the electrode charges. When the size effect of the redox ions is also considered, the current show considerable diminishment (dash lines), and the diminishment magnitude is larger at the 2 nm electrode. These results indicate that the EDL effect on the voltammetric responses for cation reduction would be significantly overestimated when ignoring the finite sizes of the redox ions. At very small electrodes (< 10 nm radii), the electrode edge effect further weaken the EDL effect.

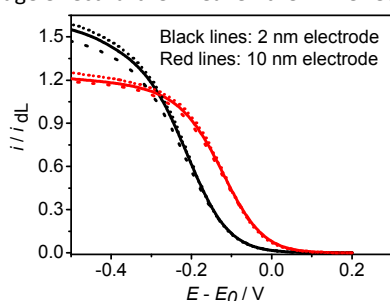


**Fig. 7** Steady-state voltammetric responses of 10 and 2 nm electrodes for reduction of a cation with +1 charge, calculated with the model considering the EDL effect and no ion size effect (solid lines), the model considering the EDL effect and the size effect of the electrolyte ions (dotted lines), and the model considering the EDL effect and the size effects of both the electrolyte and redox ions (dotted lines). The ion radii are 0.68 nm.

#### Further discussions.

The two ion radii considered here, namely, 0.38 nm and 0.68 nm, could represent the sizes of commonly used aqueous electrolyte ions (e.g., the solvated  $K^+$ ) and the organic electrolyte ions (e.g., the solvated  $TEA^+$ ) respectively. The concentration of 0.1 M considered here is also commonly employed for the supporting electrolyte in electrochemical measurements. For ions with 0.38 nm radius, as can be seen in Fig. 5a and 6a, the current deviation magnitudes due to the ion size effect are actually very small, which could be within the errors in usual measurements. This seems to suggest that the ion sizes on the voltammetric responses of nanoelectrodes in usual aqueous system can be ignored. Therefore, one can simply use the conventional PNP equations to model the mass transport of redox ions. For 0.68 nm radius ions, the ion size could visibly affect the voltammetric responses of electrodes with radii smaller than 100 nm for anion reduction (Fig. 5b) and smaller than 10 nm for cation reduction (Fig. 6b and ); and in other cases, the ion size effects would be also negligible.

The magnitudes of the ion size effects could be increased at some conditions that are not considered here. It is known from previous studies that the EDL effect would become more pronounced for reactions with lower  $k^0$  values and that with  $E^0$

values more deviating from the potential of zero charge (PZC).<sup>1,3,4</sup> In current study, we have considered the reactions with a relatively facile kinetics ( $k^0=1 \text{ cm}\cdot\text{s}^{-1}$ ). For reactions with smaller  $k^0$ , one should expect more pronounced ion size effect. We also have assumed that  $E^0=0$  (vs PZC) in current study. Usually, the standard electrode potential of a reaction should deviate from the PZC, which makes the electrode surface relatively heavily charged. This can also result in pronounced ion crowding and EDL effects, and therefore increase the magnitude of the ion size effects. Finally, the electrochemical systems considered in current study consist of relatively low concentration of electrolyte ( $0.1 \text{ mol}\cdot\text{L}^{-1}$ ) in solvents. For systems dominated with electrolyte, for examples, ionic liquids, molten salts and water-in-salts<sup>[22]</sup>, the ion size effects should become much more pronounced because the screening of electrode charges by solvent are absent. We are currently studying the ion size effect on the EDL structure and reactivity at nanoelectrodes under these conditions and situations.

## Conclusions

Modified Boltzmann and Nernst-Planck (NP) equations have been combined with the Poisson and modified Butler-Volmer equations to investigate the finite size effects of ions on the EDL structures and voltammetric responses of nanodisk electrodes. The results have shown that the ion size effect would become more pronounced for larger ions and at smaller electrodes as the electrode radii is larger than 10 nm. For electrode with radii smaller than 10 nm, however, the ion size effect becomes less pronounced due to the increased edge effect of disk electrodes at nanometer scales, which could relax the ion crowding at/near the OHP. The ion sizes on the voltammetric responses of nanoelectrodes in usual aqueous electrochemical system may be ignored. Therefore, one can use the conventional PNP equations to model the mass transport of redox ions. For 0.68 nm radius ion, which may represent some cations in organic electrolyte, the ion size may visibly affect the voltammetric responses of electrodes with radii smaller than 100 nm for anion reduction and smaller than 10 nm for cation reduction. The EDL effect on the voltammetric responses for cation reduction would be significantly overestimated when ignoring the finite sizes of the redox ions; while it will be underestimated for anion reduction.

## Acknowledgements

This work is supported by the Ministry of Science and Technology of China under the National Basic Research Program (2012CB932800) and the National Natural Science Foundation of China (21173162).

## Notes and references

- 1 S. L. Chen, Y.W. Liu and J. X. Chen, *Chem. Soc. Rev.*, 2014, **43**, 5372-5386.

- 2 S. L. Chen, Y.W. Liu, *Phys. Chem. Chem. Phys.*, 2014, **16**, 635-652.
- 3 (a) J. D. Norton, H. S. White and S. W. Feldberg, *J. Phys. Chem.*, 1990, **94**, 6772-6780. (b) C. P. Smith, H. S. White, *Anal. Chem.* 1993, **65**, 3343-3353. (c) E. J. F. Dickinson and R. G. Compton, *J. Phys. Chem. C*, 2009, **113**, 17585-17589.
- 4 (a) R. He, S. L. Chen, F. Yang, and B. L. Wu, *J. Phys. Chem. B*, 2006, **110**, 3262-3270. (b) Y.W. Liu, S. L. Chen, *J. Phys. Chem. C*, 2012, **116**, 13594-13602. (c) Y. W. Liu, R. He, Q. F. Zhang and S. L. Chen, *J. Phys. Chem. C*, 2010, **114**, 10812-10822.
- 5 (a) J. J. Watkins, J. Y. Chen, H. S. White, H. D. Abruña, E. Maisonhaute and C. Amatore, *Anal. Chem.* 2003, **75**, 3962-3971. (b) J. J. Watkins and H. S. White, *Langmuir*, 2004, **20**, 5474-5483; (c) J. L. Conyers and H. S. White, *Anal. Chem.*, 2000, **72**, 4441-4446.
- 6 D. Krapf, B. M. Quinn, M.Y. Wu, H. W. Zandbergen, C. Dekker, and S. G. Lemay, *Nano Lett.* 2006, **6**, 2531-2535.
- 7 Y. Sun, Y.W. Liu, Z.X. Liang, L. Xiong, A. L. Wang, and S. L. Chen, *J. Phys. Chem. C* 2009, **113**, 9878-9883.
- 8 (a) J. T. Cox and B. Zhang, *Annu. Rev. Anal. Chem.*, 2012, **5**, 253-272; (b) S. M. Oja, M. Wood and B. Zhang, *Anal. Chem.*, **85**, 473-486.
- 9 C. J. Slevin, N. J. Gray, J. V. Macpherson, M. A. Webb and P. R. Unwin, *Electrochem. Commun.* 1999, **1**, 282-288.
- 10 B. Zhang, L. X. Fan, H. W. Zhong, Y. W. Liu and S. L. Chen, *J. Am. Chem. Soc.*, 2013, **135**, 10073-10080.
- 11 J. J. Bikerman, *Philos. Mag.* 1942, **33**, 220, 384-397.
- 12 I. Borukhov, D. Andelman, H.Orland, *Phys. Rev. Lett.*, 1997, **79**, 435-438..
- 13 A. A. Kornyshev, *J. Phys. Chem. B*, 2007, **111**, 5545-5557.
- 14 M. S. Kilic, M. Z. Bazant, A. Ajdari, *Physical Review E: Statistical, Nonlinear, and Soft Matter Physics*, 2007, **75**(2-1), 021503/1-021503/11.
- 15 P. H. R. Alijó, F. W.Tavares, E. C. Biscaia Jr., *Colloids Surfaces A*, 2012, **412**, 29-35.
- 16 C. Liu, B. Eisenberg, *J. Phys. Chem. B*, 2012, **116**, 11422-11441.
- 17 W. Wang, S. Vince, Energy storage Redox flow batteries go organic, *Nature Chemistry*, 2016, **8**, 3, 204-206.
- 18 J. Mindemark, L. Edman, *J. Mater. Chem. C*, 2016, **4**, 420-432.
- 19 C. C. Qi, Y. X. Hua, C. Y. Xu, J. Li, Q. B. Zhang, Y. Dylan Li, *General Review*, 2014, **14**, 4, 694-707.
- 20 S. Kondrat, P. Wu, R. Qiao and A. A. Kornyshev, *Nat Mater*, 2014, **13**, 4, 387-93.
- 21 V. Giordani, D. Tozier, H. J. Tan, C.M. Burke, B.M. Gallant, J. Uddin, J. R. Greer, B. D. McCloskey, G. V. Chase, D. Addison, *J. Am. Chem. Soc.*, 2016, **138**, 8, 2656-2663.
- 22 L. M. Suo, O. Borodin, T. Gao, M. Olguin, J. Ho, X.L. Fan, C. Luo, C.S. Wang, K. Xu, *science*, 2015, **350**, 6263, 938-943.
- 23 H. N. Wang, A. Thiele, and L. Pilon, *J. Phys. Chem. C*, 2013, **117**, 36, 18286-18297.
- 24 S. Lamperski, C.W. Outhwaite, L. B. Bhuiyan, *Molecular Physics*, 1996, **87**, 5, 1049-1061.
- 25 M. Z. Bazant, M. S. Kilic, B. D. Storey, A. Ajdari, *Adv. Colloid Interfac.*, 2009, **152**, 48-88.
- 26 R. P. Buck, *J. Membr. Sci.*, 1984, **17**, 1-62.